AJNR

Prevalence of Rathke's Cleft and Other Incidental Pituitary Gland Findings on Contrast-Enhanced 3D Fat-Saturated T1-MPRAGE at 7 Tesla MRI

Mikael Mir, Nathaniel P. Miller, Matthew White, Wendy Elvendahl, Ayca Ersen Danyeli and Can Özütemiz

AJNR Am J Neuroradiol published online 24 June 2024
http://www.ajnr.org/content/early/2024/06/24/ajnr.A8393

Published June 24, 2024 as 10.3174/ajnr.A8393

ORIGINAL RESEARCH

Prevalence of Rathke's Cleft and Other Incidental Pituitary Gland Findings on Contrast-Enhanced 3D Fat-Saturated T1-MPRAGE at 7 Tesla MRI

Mikael Mir[1], Nathaniel P. Miller[1], Matthew White[2], Wendy Elvendahl[2], Ayca Ersen Danyeli[3], Can Özütemiz[4]

ABSTRACT

BACKGROUND AND PURPOSE: A cleft-like non-enhancing hypointensity was observed repeatedly in the pituitary gland at the adenohypophysis/neurohypophysis border on contrast-enhanced 3D-Fat-Saturated T_1-MPRAGE (C+3D-FS-T_1 MPRAGE) using clinical 7T MRI. Our primary goal is to assess the prevalence of this finding. The secondary goals are to evaluate the frequency of other incidental pituitary lesions, MRI artifacts, and their effect on pituitary imaging on the C+3D-FS-T_1 MPRAGE at 7T.

MATERIALS AND METHODS: 100 patients who underwent 7T neuroimaging between 10/27/2021 and 8/10/23 were included. Each case was evaluated for cleft-like pituitary hypointensity, pituitary masses, and artifacts on C+3D-FS-T_1 MPRAGE. Follow-up exams were evaluated if present. The average prevalence for each finding was calculated, as were descriptive statistics for age and sex.

RESULTS: A cleft-like hypointensity was present in 66% of 7T MRIs. There were no significant differences between the "cleft-like present" and "cleft-like absent" groups regarding sex (*P = .39*) and age (*P = .32*). The cleft-like hypointensity was demonstrated in follow-up MRIs in 3/3 patients with 7T, 1/12 with 3T, and 1/5 with 1.5T. A mass was found in 22%, while 75% had no mass, and 3% were indeterminate. A mass was found in 18 (27%) of the "cleft-like present" and 4 (13%) of the "cleft-like absent" groups. The most common mass types were Rathke cleft cyst (RCC) in 7 (31.8%) patients, "RCC vs. entrapped CSF" in 6 (27.3%), and microadenoma in 6 (22.2%) in the "cleft-like present" group. There were no significant differences in the mass types between the "cleft-like present" and "cleft-like absent" groups (*P = .23*). Susceptibility and/or motion artifacts were frequent in general using C+3D-FS-T_1 MPRAGE (54%). Artifact-free scans were significantly more frequent in the "cleft-like present" group (*P =.03*).

CONCLUSIONS: A cleft-like non-enhancing hypointensity was frequently seen on the C+3D-FS-T1 MPRAGE at 7T MRI, which most likely represents a normal embryological Rathke's cleft remnant and cannot be seen in lower field strength MRIs. Susceptibility and motion artifacts are common in the sella. They may affect image quality, and the artifacts at 7T may lead to an underestimation of the prevalence of Rathke cleft and other incidental findings.

ABBREVIATIONS: C+3D-FS-T_1MPRAGE = Contrast-Enhanced 3D-Fat-Saturated T_1- Magnetization Prepared Rapid Gradient Echo Imaging; RCC = Rathke's Cleft Cyst.

Received month day, year; accepted after revision month day, year.
[1] University of Minnesota Medical School, Minneapolis, MN, United States
[2] Center for Magnetic Resonance Research, University of Minnesota, Minneapolis, MN, United States
[3] Acıbadem University, School of Medicine, Department of Pathology, Istanbul, Turkey
[4] University of Minnesota Medical School, Department of Radiology, Minneapolis, MN, United States

The authors declare no conflicts of interest related to the content of this article. This study was presented as an electronic poster at the 2024 ASNR meeting.

Please address correspondence to Dr. Can Özütemiz, Department of Radiology, University of Minnesota, MMC 292, 420 Delaware St. SE Minneapolis, MN 55455, USA
Phone: +1-612-626-5566
Email: ozutemiz@umn.edu
X: @CanOzutemiz

SUMMARY SECTION

PREVIOUS LITERATURE: 7T MRI offers better spatial resolution, which has improved discrimination of small lesions and anatomy. In our daily practice, we have repeatedly observed a cleft-like J-shaped or C-shaped non-enhancing hypointensity in the pituitary gland at the adenohypophysis/neurohypophysis border on sagittal C+3D-FS-T1 MPRAGE at 7T. Gobara et al. observed a belt-like T2 hypointensity in the posterior margin of the adenohypophysis in 37.7% of 212 cases on T2-weighted images at 3T MRI, and the investigators postulated that this represented "pars intermedia" or Rathke's cleft remnant. This benign embryological remnant can further develop into a large Rathke's cleft cyst.

KEY FINDINGS: A cleft-like pituitary hypointensity was present in 66/100 (66%) patients. This incidental finding was demonstrated in 3/3 patients with 7T, 1/12 with 3T, and 1/5 with 1.5T follow-up. A pituitary mass was found in 22%, and susceptibility and/or motion artifacts were generally frequent (54%) when using C+3D-FS-T1 MPRAGE at 7T.

KNOWLEDGE ADVANCEMENT: A cleft-like non-enhancing hypointensity is frequently present on C+3D-FS-T1 MPRAGE at 7T MRI. This is likely benign Rathke's cleft remnant and cannot be seen in lower field strength MRIs. Susceptibility and motion artifacts are common in the sella, which may affect image quality at 7T.

Copyright 2024 by American Society of Neuroradiology.

INTRODUCTION

The FDA has approved 7T MRI machines for clinical knee and brain imaging using dedicated coils[1-3]. 7T MRI technology offers several advantages over conventional 1.5 and 3T MRI systems, including a higher signal-to-noise ratio and contrast-to-noise ratio, which provide MR images with better spatial resolution, improving discrimination of smaller lesions and anatomy[3-6]. Conversely, 7T MRI technology brings new challenges. The primary limitations in clinical 7T neuroimaging are transit B_1-field inhomogeneities and increased susceptibility effects, which limit imaging of the skull base[3-5, 7-13]. Another limitation is increased sensitivity to motion and pulsation artifacts[3, 9, 10]. Despite these limitations, 7T MRI has been shown to detect small pituitary microadenomas, occult on conventional pituitary MRI at lower field strengths[3, 14-18].

7T MRI has been used at our center since 2020 for various indications, including pituitary imaging. We routinely obtain a sagittal acquired contrast-enhanced 3D-fat-saturated T_1-MPRAGE (C+3D-FS-T_1 MPRAGE) with axial and coronal reformats for post-contrast brain imaging at 7T, which is the main contrast-enhanced sequence we use to evaluate contrast-enhancing intracranial pathologies. In our daily practice, we have repeatedly observed "a cleft-like J-shaped or C-shaped non-enhancing hypointensity in the pituitary gland at the border of the adenohypophysis and neurohypophysis on the C+3D-FS-T_1 MPRAGE sequence, best appreciated in the sagittal plane. In this study, our primary goal is to determine the prevalence of this finding and assess whether it is visualized on follow-up MRIs with either 7T or lower field strengths. Our second goal is to evaluate the frequency of other incidental pituitary gland lesions, MRI artifacts, and their effect on pituitary imaging on the C+3D-FS-T_1 MPRAGE sequence at 7T.

MATERIALS AND METHODS

This study protocol was approved by the Institutional Review Board at the University of Minnesota. Given the study's retrospective nature, the IRB granted a waiver for informed consent.

Image Acquisition and Interpretation

Images and demographic data from 175 patients who underwent neuroimaging with an FDA-approved clinical 7T MRI scanner (Siemens Magnetom Terra, Erlangen, Germany) equipped with a 1-channel transmit/32-channel receive head coil (Nova Medical, Wilmington, USA) at the Center for Magnetic Resonance Research in Minneapolis, MN between 10/27/2021 and 8/10/23 were collected for this study. Our C+3D-FS-T1 MPRAGE sequence parameters are shown in Table-1. A half dose (0.05cc/kg) of standard gadolinium contrast agent (Gadavist, Bayer, Leverkusen, Germany) is applied routinely for each 7T MRI exam at our center. Calcium-titanate dielectric pads were placed in the sub-occipital and pre-auricular regions, depending on the patient's head size. We specifically apply these pads because transmit B1 inhomogeneities may limit the visibility of nearby structures at the cranium base with 7T and dielectric pads were proven to decrease these effects3, 19, 20. The following clinical data were collected: age, gender, and exam indication.

Each case was evaluated for two findings on C+3D-FS-T1 MPRAGE: A cleft-like J-shaped or C-shaped non-enhancing pituitary hypointensity at the border of the adenohypophysis and neurohypophysis (cleft-like present) and a pituitary gland mass, scored as absent, present, or indeterminate. The presence of a posterior pituitary T1 bright spot, consistent with neurohypophysis, was assessed in the pre-contrast and post-contrast MPRAGE series, and they were scored as absent, present, indeterminate, or ectopic. The presence and type of artifacts seen on C+3D-FS-T1 MPRAGE were also recorded. Data from those with prior or follow-up scans were collected as well. The voxel size of our institutional C+3D-T1 MPRAGE at 1.5 T and 3T MRI is 1x1x1 mm.

Data Analysis and Statistics

After an initial training session, which included 20 cases provided by a board-certified neuroradiologist (6 years of experience and >2 years of experience reading a high volume of clinical 7T MRI cases), two medical students evaluated and assessed all 175 7T MRI exams. Seventy-five cases were excluded from the final analysis due to a lack of C+3D-FS-T1 MPRAGE sequence (73) or motion artifact limiting interpretation (2). A total of 100 MRIs were included. Then, the attending neuroradiologist separately reviewed and controlled all included cases in a separate session, either agreeing or disagreeing with the medical students to reach a final consensus agreement.

The average and standard deviation for each of the three findings were calculated from the remaining cases and descriptive statistics for age, sex, protocol, and indication. To assess for differences in baseline demographic characteristics between the "cleft-like present" and "cleft-like absent " groups, a Chi-squared test was performed to evaluate for differences in sex, and an unpaired, two-tailed t-test was performed to evaluate for differences in patient age. Additional Chi-squared testing was conducted to assess differences in the type of masses, presence, and type of artifacts in the two groups. A subgroup analysis was performed for patients with follow-up C+3D-FS-T_1 MPRAGE at any field strength.

RESULTS

Among the 100 patients included, 64 were female and 36 were male, with an average age of 47.3 ± 18.9 years. The indications for each study used in the cohort are shown in Table-2 .

A cleft-like pituitary hypointensity was present in 66 (66%) patients, absent in 31 (31%), and indeterminate in 3 (3%) (Fig. 1, Fig. 2, Fig. 3). Indeterminate cases were excluded from subsequent analyses. For the "cleft-like present" group, 41 (62%) were female, and 25 (38%) were male, with an average age of 46.1 ± 19.9 years. For the "cleft-like absent" group, 22 (71%) were female, and 9 (29%) were male, with an average age of 50.3 ± 17.1. There were no significant differences in the baseline characteristics of the "cleft-like present" and "cleft-like absent" groups regarding sex ($X^2(1, n = 97) = 0.73$, $P = .39$) or age (two-tailed t-test; $P = .32$). In the "cleft-like present" group, 20 patients underwent follow-up imaging. A cleft-like hypointensity in the pituitary gland was demonstrated in 3/3 patients with

7T, 1/12 with 3T, and 1/5 with 1.5T follow-up (Fig. 2, Fig. 3).

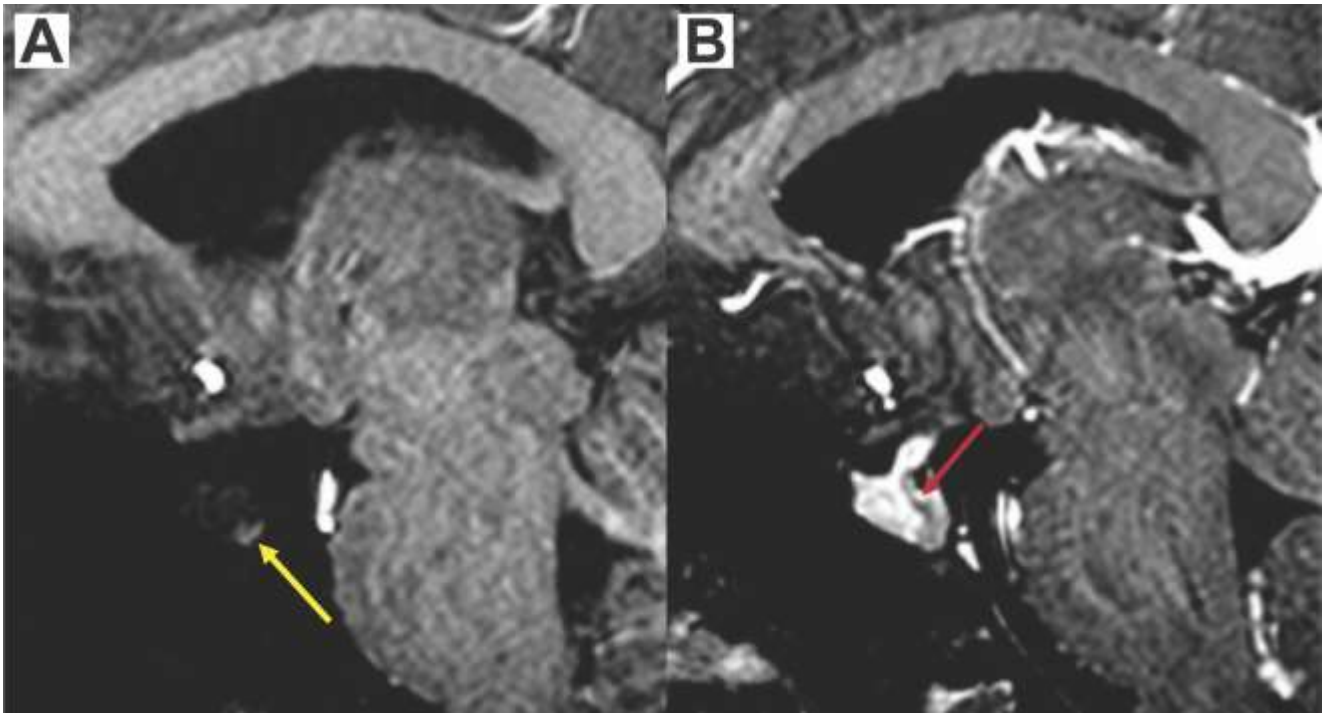

Figure 1. A 32-year-old female who was scanned for multiple sclerosis follow-up. **A)** Pre-contrast 3D-FS-T_1 MPRAGE shows a very dark adenohypophysis and stalk. A posterior T_1 bright spot is present (yellow arrow). **B)** Post-contrast image shows diffuse homogeneous enhancement of the stalk, adenohypophysis, and an incidental curved non-enhancing hypointensity (red arrow), extending from the stalk between the vicinity of adenohypophysis and neurohypophysis, presumably representing the Rathke's cleft.

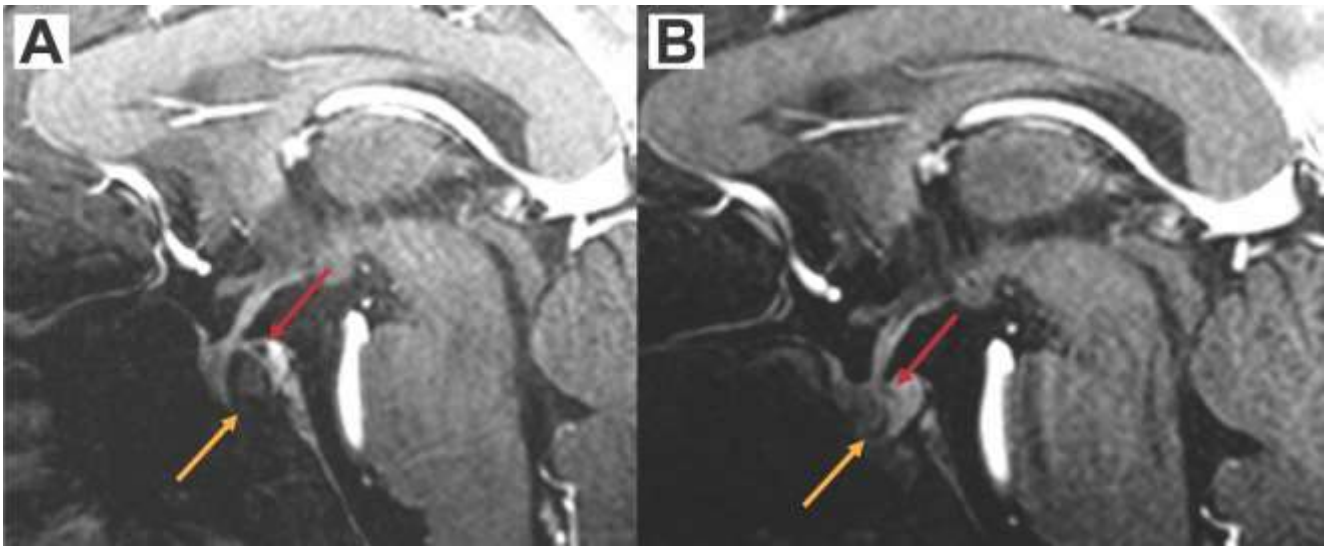

Figure 2. A) A 30-year-old male with pituitary hypofunction. On a sagittal post-contrast 3D-FS-T_1 MPRAGE at 7T, the orange arrow shows a biopsy-proven large Rathke cleft cyst, and the red arrow shows a separate triangular-shaped hypointensity more posterior and superior to the cyst. **B)** A 3-month follow-up with 7T MRI after endoscopic transsphenoidal drainage of the cyst shows a decompressed Rathke cleft cyst (orange arrow) and a more dilated and prominent appearance of the J-shaped cleft-like presumed Rathke's cleft (red arrow), likely due to resolution of mass effect. Pituitary hypofunction resolved after the surgery.

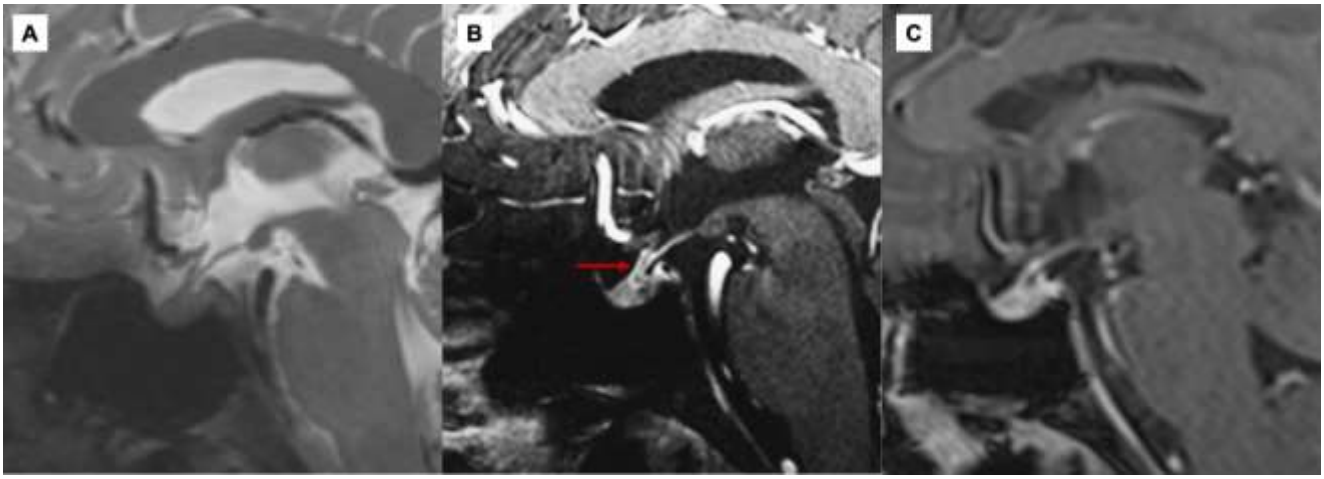

Figure 3. A 37-year-old male with medically refractory epilepsy and prior temporal lobectomy was referred to 7T MRI for follow-up. **A)** Sagittal pre-contrast 3D-T_2-SPACE does not show any abnormality in the pituitary gland, and the lesion pointed out with the red arrow in **B** is not visible. **B)** Sagittal post-contrast 3D-FS-T_1 MPRAGE at 7T shows string-like C-shaped hypointensity extending from the stalk all the way through the adenohypophysis (red arrow), favored as Rathke's cleft. **C)** Sagittal contrast-enhanced 3D T1 MPRAGE images obtained 5 months later at 3T MRI are unable to demonstrate the presumed Rathke's cleft.

A mass-like appearance in the pituitary gland was found in 22 (22%) patients, while 75 (75%) had no mass, and 3 (3%) were indeterminate. The most common types of masses in the "cleft-like present" group were Rathke cleft cyst (RCC) in 7 (31.8%) patients, "RCC vs. entrapped CSF" in 6 (27.3%), and pituitary adenoma in 6 (22.2%). In the "cleft-like absent" group, only 20% of patients had an "RCC vs entrapped CSF" like appearance and no RCC was identified radiologically. Some patients had two masses noted on their interpretation, and the prevalence of all masses noted is shown in Table-3. There was no significant difference in the types of mass present in the "cleft-like present" and "cleft-like absent" groups ($X^2(6, n = 27) = 8.06$, $P = .23$). A posterior T_1 bright spot was present in 93 (93%) patients, absent in 3 (3%), indeterminate in 3 (3%), and ectopic in 1 (1%) at the stalk. Posterior T_1 bright spot was present in the expected area in 94% of patients in the "cleft-like present" group (62/66) and 94% in the "cleft-like absent" (29/31).

Regarding artifacts, 54 (54%) patients had some type of artifact noted in the C+3D-FS-T_1 MPRAGE, and the prevalence of artifacts within the cohort is outlined in Table-4.

DISCUSSION

Our results characterize a previously unreported cleft-like J-shaped/C-shaped non-enhancing pituitary hypointensity found on C+3D-FS-T1 MPRAGE in most patients scanned at 7T. This finding was specifically localized between the T1 hyperintense neurohypophysis and the adenohypophysis, which appears T1 hypointense on the pre-contrast series and homogeneously enhancing in the post-contrast series (Fig. 1). While this incidental observation was repeatedly noted in a small group of patients with available follow-up at 7T, it was not appreciated in most cases with lower field strength follow-ups or could be identified in the lower field strengths only after initially seeing the lesion at 7T. This incidental imaging finding presumably represents a tiny true anatomic structure that is only visible with 7T and obscured in lower field strengths due to relatively lower spatial and contrast resolution. The frequency of this J-shaped cleft-like hypointensity may also be underestimated in our series, as a significantly greater proportion of patients in the "cleft-like absent" group had artifact-degraded studies, which may have limited visualization.

After correlation with histopathologic examinations from cadavers and pituitary tumor resections, we concluded that this cleft-like hypointensity presumably represents Rathke's cleft, an embryological remnant of Rathke's pouch (Fig. 4), seen as a normal anatomical structure between pars intermedia and pars distalis, which is not typically observed in lower strength studies[21-24]. Embryologically, Rathke's pouch is derived from the ectodermal buccopharyngeal membrane and grows dorsally at around three weeks of gestation. At approximately 32 days, this structure is disconnected from the oral cavity and communicates with the diencephalon. At the same time, the infundibular process grows from the diencephalon inferiorly towards the buccal cavity to form the neurohypophysis and the stalk. The anterior wall of the Rathke pouch forms the adenohypophysis, and the posterior wall forms the pars intermedia[21, 22]. Sometimes, Rathke's pouch leaves a remnant between the pars distalis and pars intermedia, known as Rathke's cleft, which can further develop into a large RCC[21, 22]. Note that RCC and "cyst of the pars intermedia" are two terms used interchangeably in the literature, and a true differentiation of those two is unclear.

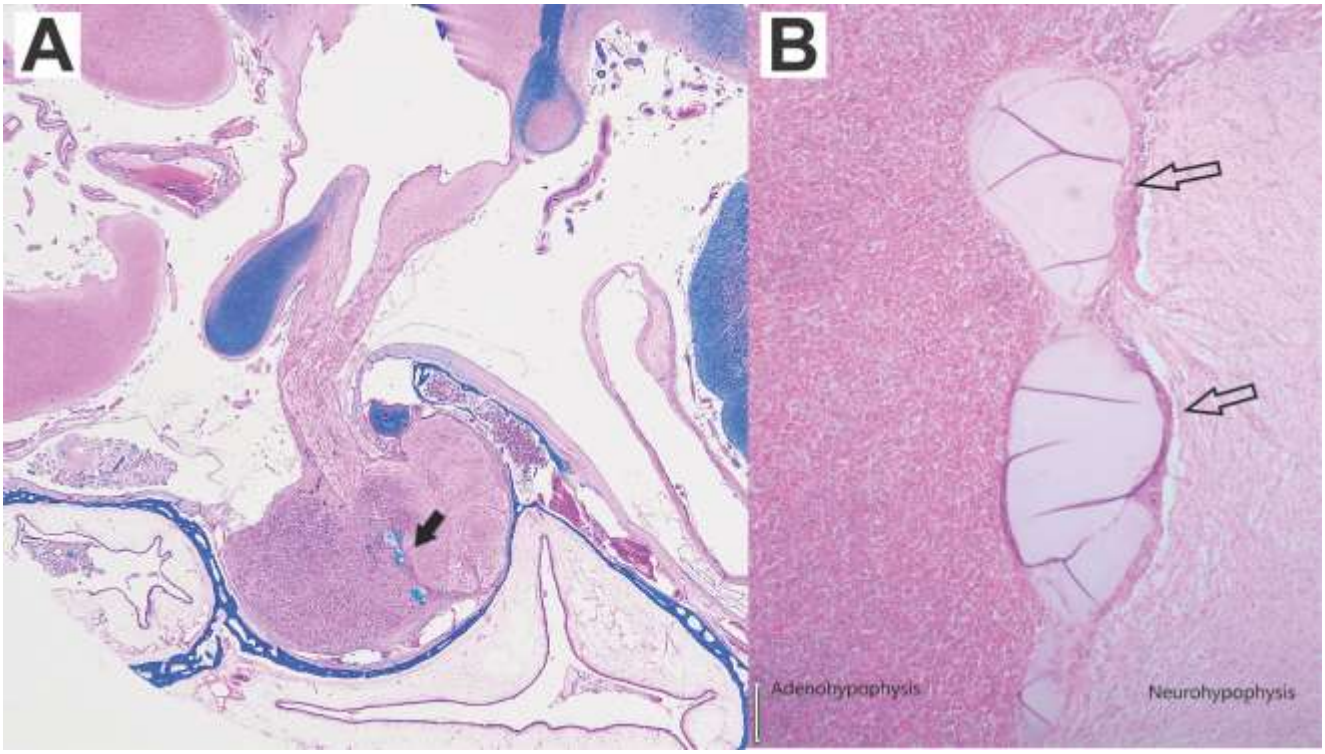

Figure 4. A) The whole-slide image from an autopsy case shows the pituitary gland along with anatomically adjacent tissues. The arrow indicates Rathke's cleft remnant (Stained with Luxol fast blue combined with periodic acid-Schiff, 0.5X magnification). **B)** The closer view depicts Rathke's cleft remnant (arrows) (Stained with Hematoxylin and Eosin, 20X magnification).

To our knowledge, Gobara et al.'s study is the only one with a similar and interesting observation[26]. In this study, the investigators obtained high-resolution 2D T2-TSE images of the pituitary gland at 3T. They observed a T2 hypointensity in the posterior margin of the adenohypophysis in 37.7% of 212 cases, of which 37 (17.5%) showed a belt-like hypointensity on T2 weighted images, and the investigators postulated that this belt-like T2 hypointense radiologic observation represented "pars intermedia" or Rathke's cleft remnant, similar to us[26]. In our routine 7T MRI protocols, we do not acquire a high-resolution 2D TSE sequence focused on the pituitary gland. Thus, we did not analyze how here-described cleft-like J-shaped/C-shaped non-enhancing hypointensity appeared in T2 weighted images. However, in our 7T study, the prevalence of this incidental finding is even higher compared with the findings of Gobara et al. (66% vs 17.5%).

The prevalence of RCC in our cohort was 7%. The true prevalence of RCCs in the general population is variable in the literature. Since symptomatic cases are rare, many RCCs are found postmortem. Autopsy studies suggest that the prevalence is between 13-23%, with some studies finding incidental lesions in 11% of postmortem cases[27, 28]. Regarding radiological prevalence, the prevalence of RCC on MRI was found at 3% in the pediatric population, and one study performed in a tertiary pituitary center including all age groups found a prevalence of 3.4% in 2598 pituitary MRI cases using conventional 1.5 and 3T MRI machines[29, 30].The prevalence in our small cohort is greater than the latter radiology report, probably due to improved spatial and contrast resolution at 7T but is still less than the prevalence reported by the autopsy studies. Regardless, RCCs are benign incidental cysts that are often asymptomatic and only rarely cause endocrinologic dysfunction when they are sufficiently large to have a mass effect on adjacent structures[25, 31]. Despite the lack of statistical difference, in almost a quarter of the "cleft-like present" patients, an RCC was present, while none in the "cleft-like absent" group had an RCC. This relationship increases the potential association between the visible Rathke cleft remnant and RCC (Table-3).

It is known that RCC may appear similar to a non-enhancing cystic pituitary adenoma, and radiological differentiation is sometimes impossible[22, 24]. With the improved resolution gained with 7T imaging, we could identify additional mass-like structures in these C+3D-FS-T1 MPRAGE sequences. One was presumed to represent entrapped CSF underneath the diaphragma sellae or CSF-filled arachnoid indentations into the adenohypophysis. Unlike RCC, these non-enhancing cyst-like structures were almost always off the midline in unexpected locations for RCC, either lateral or superior lateral to the adenohypophysis, demonstrating a similar signal to CSF, and usually contiguous with the CSF, as seen in Fig. 5. As shown in Table-3, in a few cases, we were unable to differentiate the nature of the cyst. Therefore, we debated whether these were incidental non-enhancing adenomas, RCCs, or entrapped CSF. As we are in the early stages of clinical usage of 7T MRI, neuroradiologists are not used to depicting subtle pituitary pathologies at 7T, even in the most experienced institutions with high volumes of 7T MRI. As such, it is important for those interpreting these studies to understand the appearance of Rathke's cleft remnant, RCC, and other incidental benign cystic lesions, such as entrapped CSF underneath the diaphragma sellae or CSF-filled arachnoid indentations, and to differentiate these from other pituitary lesions, such as microadenomas, to avoid unnecessary follow-up laboratory testing and imaging for the patient[31].

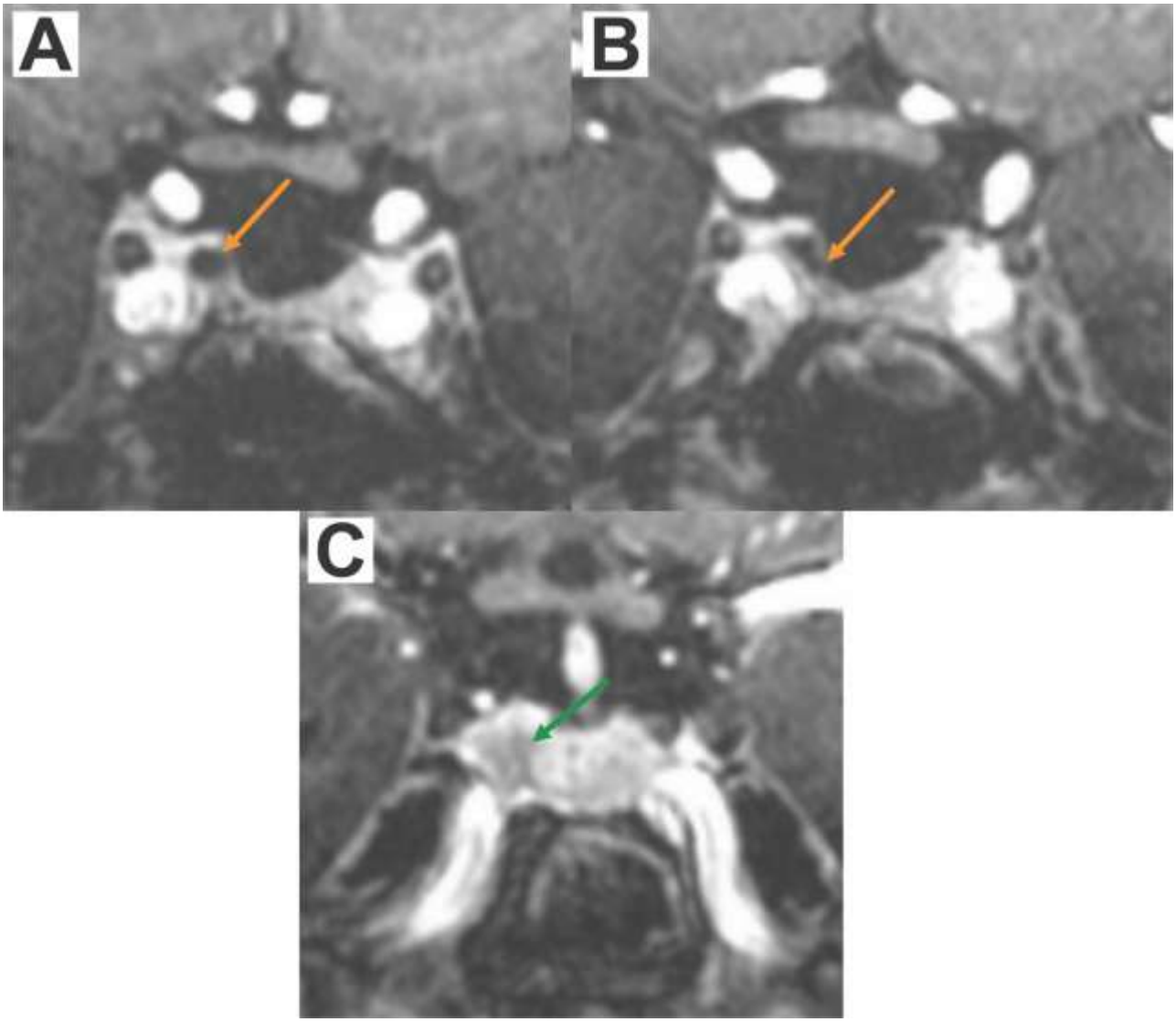

Figure 5. A 45-year-old female with increased prolactin levels who had a transnasal endoscopic pituitary adenoma resection and underwent a follow-up with a 7T MRI due to increased prolactin levels two months after the surgery. **A)** Coronal post-contrast 3D-FS-T1 MPRAGE shows a hypointense cystic structure mimicking a cystic adenoma located at the right ventral aspect of the adenohypophysis (orange arrow) with indistinct margins. **B)** When scrolled posteriorly, the cystic mass connects with CSF. Thus, this was favored to be entrapped CSF in the operation field. **C)** When scrolled even further in the posterior direction, there was a more hypointense focus with indistinct margins in the right aspect of the adenohypophysis, considered as a residual adenoma (green arrow).

High-resolution post-contrast 3D-T1-MPRAGE at 7T was recently found to be more successful in identifying pituitary microadenomas in a small cohort of Cushing patients compared with other 3D, 2D, and dynamic sequences[18]. Sphenoid sinus pneumatization is also reported as a limiting factor because of increased susceptibility artifacts in the air-bone interphase[18]. Our institutional experience aligns with the report from this group. In most of the scans in our sample, some degree of artifact was noted, either motion-related or susceptibility artifact, mainly occurring in the sella floor from the air-bone interphase or B1-field inhomogeneities (Fig. 6, Fig. 7). Motion artifacts are a known problem, with scans requiring a longer acquisition time, and it is known that artifacts are exaggerated at 7T compared with conventional MRIs at 1.5T and 3T[3]. There were significantly more artifact-free scans in the "cleft-like present" group than in the "cleft-like absent" group, implying that the higher degree of artifact in the "cleft-like absent" group could have limited our ability to identify the J-shaped/C-shaped cleft-like hypointensity. Thus, it is possible the overall prevalence of the cleft-like hypointensity is relatively underestimated in our cohort (Table-4).

Figure 6. A 19-year-old female was imaged for a low-grade brain tumor at 7T. While the cleft-like presumed Rathke's Cleft remnant can be depicted (red arrow), pulsation artifact from the adjacent basilar artery (blue arrow) and susceptibility artifact associated with sphenoid sinus (blue arrowhead) limits the assessment of the ventral and inferior portions of the pituitary gland.

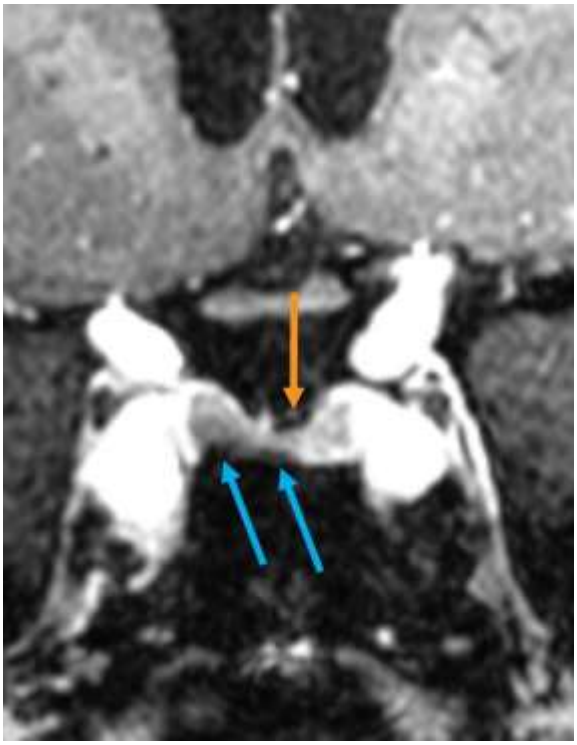

Figure 7. An 83-year-old female who was referred for a brain MRI for a posterior communicating artery aneurysm follow-up. Coronal C+3D-FS-T_1 MPRAGE shows round-shaped susceptibility artifacts in the base of the adenohypophysis (blue arrows), which may mimic a hypointense adenoma and limit the assessment of the base. A cystic-appearing T1 hypointense area immediately lateral to the stalk and superior to the gland (orange arrow) is separated by a thin membrane and is continuous with adjacent CSF in other slices (not shown). This was favored to represent an entrapped CSF between the gland and the diaphragm, mimicking a cystic mass.

One of the limitations of this study is the lack of pathologic confirmation in our cohort. While this is potentially a limitation, within the limits of a retrospective study with incidental benign findings seen on 7T MRI, it is inhumane and impractical to perform pathologic confirmation. In order to decrease this limitation, we correlated our imaging with prior autopsy cases. An autopsy case in the

future with available prior contrast-enhanced 7T MRI may confirm our findings. Another minor limitation is that all images were first assessed by medical students and their observations were corrected by a single experienced neuroradiologist. Therefore interobserver variability analysis was not made.

Table 1: C+3D-FS-T_1 MPRAGE sequence parameters.

Parameter	Value
Plane	Sagittal
Slice Thickness (mm)	0.6
Matrix	224 x 224
FOV (mm)	150
Interslice Distance (%)	50
Voxel Size (mm^3)	0.3 x 0.3 x 0.3*
Acquisition Time (min)	6:32
TR/TE (ms)	3000/2.49

*****In our contrast-enhanced radiotherapy protocol, the interpolation is off to decrease geometric distortion, and therefore the voxel size is 0.6 x 0.6 x 0.6 mm^3

Table 2: 7T MRI indications.

Indication	n, %
Epilepsy	10 (10%)
Headache	10 (10%)
Multiple sclerosis	8 (8%)
Pituitary adenoma	8 (8%)
Seizure	6 (6%)
Pituitary lesion	5 (5%)
Assess for CAA	4 (4%)
Brain lesion	4 (4%)
Radiotherapy planning	4 (4%)
Cushing disease	3 (3%)
Gait disorder	3 (3%)
Radiotherapy planning for glioblastoma	3 (3%)
Glioblastoma	3 (3%)
Memory changes	3 (3%)
Stroke/transient ischemic attack	3 (3%)
Vision changes	3 (3%)
Dizziness	2 (2%)

Table 3: Frequency of pituitary masses.

Mass Type	Total (n, %)	Cleft-like Present (n, %)	Cleft-like Absent (n, %)
Rathke cleft cyst	7 (25.9%)	7 (31.8%)	0
Rathke cleft cyst vs. entrapped CSF	7 (25.9%)	6 (27.3%)	1 (20%)
Rathke cleft cyst vs. entrapped CSF vs. adenoma	2 (7.4%)	2 (9.1%)	0
Entrapped CSF	3 (11.1%)	1 (4.5%)	2 (40%)
Adenoma	6 (22.2%)	4 (18.2%)	2 (40%)
Drained Rathke cleft cyst w/o mass effect	1 (3.7%)	1 (4.5%)	0
Adenoma vs artifact	1(3.7%)	1 (4.5%)	0
Total (frequency)	27	22	5
Rathke cleft cyst	7 (25.9%)	7 (31.8%)	0
Rathke cleft cyst vs. entrapped CSF	7 (25.9%)	6 (27.3%)	1 (20%)
Rathke cleft cyst vs. entrapped CSF vs. adenoma	2 (7.4%)	2 (9.1%)	0
Entrapped CSF	3 (11.1%)	1 (4.5%)	2 (40%)
Adenoma	6 (22.2%)	4 (18.2%)	2 (40%)
Drained Rathke cleft cyst w/o mass effect	1 (3.7%)	1 (4.5%)	0
Adenoma vs artifact	1(3.7%)	1 (4.5%)	0
Total (frequency)	27	22	5

Table 4: Prevalence of artifacts.*

Artifact	Total (n, %)	Cleft-like Present (n, %)	Cleft-like Absent (n, %)
Present	57 (58.8%)	34 (51.5%)	23 (74.2%)
Absent	40 (41.2%)	32 (48.5%)	8 (25.8%)
Total (patients)	97	66	31
Artifact Type			
Motion	30 (41.1%)	19 (44.2%)	11 (36.7%)
Susceptibility	43 (58.9%)	24 (55.8%)	19 (63.3%)
Total (frequency)	73	43	30

*Overall presence of artifact across patients (N = 97, 3 omitted), reported in total and for "Cleft-like Present" and "Cleft-like Absent" groups. A statistically significant difference between "Cleft-like Present" and "Cleft-like Absent" groups, with a proportionately higher rate of scan artifact in the "Cleft-like Absent" group (X^2(1, n = 97) = 4.48, P =.*03*). Below are sub-group frequencies of artifact types. Note that the bottom rows report artifact frequencies across studies, not by the patient (some scans include both susceptibility and motion artifacts). No statistically significant difference in types of artifacts between "Cleft-like Present" and "Cleft-like Absent" groups (X^2(1, n = 73) = 0.41, P = .*52*).

CONCLUSIONS

A non-enhancing, J-shaped or C-shaped, cleft-like hypointensity in the pituitary gland between the adenohypophysis and neurohypophysis is seen in most of the sagittal contrast-enhanced 3D-fat-saturated T1-MPRAGE sequences at 7T MRI. We suggest this radiologic observation represents Rathke's cleft, an embryological Rathke's pouch remnant, seen as a normal anatomical structure between pars intermedia and pars distalis on histopathology, which cannot be seen clearly at lower field strength MRIs. The artifacts at 7T are a limiting factor, and perhaps the overall prevalence of this cleft-like hypointensity is underrepresented due to the artifacts, limiting interpretation. Additionally, 7T MRI may further capture incidental benign cystic pituitary lesions, such as presumed entrapped CSF under the diaphragm sellae or arachnoid indentations into the adenohypophysis, in unexpected locations for RCC.

ACKNOWLEDGMENTS

Acknowledgments have to be in a separate section but it does not have to be a freestanding page. Obtaining permission to include a name in this section from the acknowledged individual is advised.

REFERENCES

1. FDA clears first 7T magnetic resonance imaging device. https://www.fda.gov/news-events/press-announcements/fda-clears-first-7t-magnetic-resonance-imaging-device Accessed January 11, 2023
2. Bringing Ultra-High Field MR Imaging from Research to Clinical: SIGNA 7.0T FDA Cleared. https://www.gehealthcare.com/about/newsroom/press-releases/bringing-ultra-high-field-mr-imaging-from-research-to-clinical-signa-70t-fda-cleared Accessed December 12, 2023
3. Ozutemiz C, White M, Elvendahl W, et al. Use of a Commercial 7-T MRI Scanner for Clinical Brain Imaging: Indications, Protocols, Challenges, and Solutions-A Single-Center Experience. *AJR Am J Roentgenol* 2023; 221:788-804. DOI: 10.2214/AJR.23.29342
4. Okada T, Fujimoto K, Fushimi Y, et al. Neuroimaging at 7 Tesla: a pictorial narrative review. *Quant Imaging Med Surg* 2022;12:3406-3435. DOI: 10.21037/qims-21-969
5. Opheim G, van der Kolk A, Markenroth Bloch K, et al. 7T Epilepsy Task Force Consensus Recommendations on the Use of 7T MRI in Clinical Practice. *Neurology* 2021;96:327-341. DOI: 10.1212/WNL.0000000000011413
6. Ugurbil K. Magnetic resonance imaging at ultrahigh fields. *IEEE Trans Biomed Eng* 2014;61:1364-1379. DOI: 10.1109/TBME.2014.2313619
7. Grams AE, Kraff O, Kalkmann J, et al. Magnetic resonance imaging of cranial nerves at 7 Tesla. *Clin Neuroradiol* 2013;23:17-23. DOI: 10.1007/s00062-012-0144-3
8. Lecler A, Duron L, Charlson E, et al. Comparison between 7 Tesla and 3 Tesla MRI for characterizing orbital lesions. *Diagn Interv Imaging* 2022;103:433-439. DOI: 10.1016/j.diii.2022.03.007
9. Ma R, Henry TR, Van de Moortele PF. Eliminating susceptibility induced hyperintensities in T1w MPRAGE brain images at 7 T. *Magn Reson Imaging* 2019;63:274-279. DOI: 10.1016/j.mri.2019.08.013
10. Snaar JE, Teeuwisse WM, Versluis MJ, et al. Improvements in high-field localized MRS of the medial temporal lobe in humans using new deformable high-dielectric materials. *NMR Biomed* 2011;24:873-879. DOI: 10.1002/nbm.1638
11. Teeuwisse WM, Brink WM, Webb AG. Quantitative assessment of the effects of high-permittivity pads in 7 Tesla MRI of the brain. *Magn Reson Med* 2012;67:1285-1293. DOI: 10.1002/mrm.23108
12. Van de Moortele PF, Akgun C, Adriany G, et al. B(1) destructive interferences and spatial phase patterns at 7 T with a head transceiver array coil. *Magn Reson Med* 2005;54:1503-1518. DOI: 10.1002/mrm.20708
13. Yang QX, Mao W, Wang J, et al. Manipulation of image intensity distribution at 7.0 T: passive RF shimming and focusing with dielectric materials. *J Magn Reson Imaging* 2006;24:197-202. DOI: 10.1002/jmri.20603
14. Eisenhut F, Schlaffer SM, Hock S, et al. Ultra-High-Field 7 T Magnetic Resonance Imaging Including Dynamic and Static Contrast-Enhanced T1-Weighted Imaging Improves Detection of Secreting Pituitary Microadenomas. *Invest Radiol* 2022;57:567-574. DOI: 10.1097/RLI.0000000000000872
15. Patel V, Liu CJ, Shiroishi MS, et al. Ultra-high field magnetic resonance imaging for localization of corticotropin-secreting pituitary adenomas. *Neuroradiology* 2020;62:1051-1054. DOI: 10.1007/s00234-020-02431-x
16. Rutland JW, Delman BN, Feldman RE, et al. Utility of 7 Tesla MRI for Preoperative Planning of Endoscopic Endonasal Surgery for Pituitary Adenomas. *J Neurol Surg B Skull Base* 2021;82:303-312, DOI: 10.1055/s-0039-3400222
17. Yao A, Rutland JW, Verma G, et al. Pituitary adenoma consistency: Direct correlation of ultrahigh field 7T MRI with histopathological analysis. *Eur J Radiol* 2020;126:108931 DOI: 10.1016/j.ejrad.2020.108931
18. Mark IT, Welker K, Erickson D, et al. 7T MRI for Cushing's Disease: A Single Institutional Experience and Literature Review. *AJNR Am J Neuroradiol* 2024. DOI: 10.3174/ajnr.A8209
19. Teeuwisse WM, Brink WM, Webb AG. Quantitative assessment of the effects of high-permittivity pads in 7 Tesla MRI of the brain. Magn Reson Med 2012; 67:1285-1293
20. Fagan AJ, Bitz AK, Bjorkman-Burtscher IM, et al. 7T MR Safety. J Magn Reson Imaging 2021; 53:333-346
21. Castillo M. Pituitary gland: development, normal appearances, and magnetic resonance imaging protocols. *Top Magn Reson Imaging* 2005;16:259-268. DOI: 10.1097/01.rmr.0000224682.91253.15
22. Tortori-Donati P, Rossi A, Biancheri R. Sellar and Suprasellar Disorders. In: Tortori-Donati P, ed. *Pediatric Neuroradiology* 1st ed. Heidelberg: Springer; 2005:855-892
23. Raybaud C, Barkovich AJ. Rathke Cleft Cysts. In: Raybaud C, Barkovich AJ. eds. *Pediatric Neuroimaging*. Philadelphia: Lippincott Williams & Wilkins; 2012:733-734
24. Osborn AG. Rathke Cleft Cyst. In: Osborn AG, ed. *Brain*. Manitoba, Canada: Amirsys; 2013:682-699
25. Mahdi ES, Webb RL, Whitehead MT. Prevalence of pituitary cysts in children using modern magnetic resonance imaging techniques. *Pediatr Radiol* 2019;49:1781-1787. DOI: 10.1007/s00247-019-04479-1
26. Gobara A, Katsube T, Asou H, Yoshida R, Yoshizako T, Kitagaki H. T2 hypointense signal discovered incidentally at the posterior edge of the adenohypophysis on MRI: its prevalence and morphology and their relationship to age. *Neuroradiology*. 2022;64(9):1755-1761. doi:10.1007/s00234-022-02935-8
27. Mendoza JWL, Strickland BA, Micko A, et al. Prevalence Rate of Coexisting Rathke Cleft Cysts and Pineal Cysts: A Multicenter Cross-Sectional Study. *World Neurosurg* 2021;149:e455-e459. DOI: 10.1016/j.wneu.2021.02.004

28. Larkin S, Karavitaki N, Ansorge O. Rathke's cleft cyst. In: Fliers E, Korbonits M, Romijn JA, eds. *Handbook of Clinical Neurology*. Amsterdam, Netherlands: Elsevier; 2014:255-269
29. Schmidt B, Cattin F, Aubry S. Prevalence of Rathke cleft cysts in children on magnetic resonance imaging. *Diagn Interv Imaging*. 2020;101(4):209-215. doi:10.1016/j.diii.2019.12.005
30. Famini P, Maya MM, Melmed S. Pituitary magnetic resonance imaging for sellar and parasellar masses: ten-year experience in 2598 patients. *J Clin Endocrinol Metab* 2011;96:1633-1641. DOI: 10.1210/jc.2011-0168
31. Hoang JK, Hoffman AR, González RG, et al. Management of Incidental Pituitary Findings on CT, MRI, and ^{18}F-Fluorodeoxyglucose PET: A White Paper of the ACR Incidental Findings Committee. *J Am Coll Radiol*. 2018;15(7):966-972. doi:10.1016/j.jacr.2018.03.037

SUPPLEMENTAL FILES